OPERATIONAL EXPERIENCE WITH SUPERCONDUCTING UNDULATORS AT APS*

K. C. Harkay[†], L. Boon, M. Borland, J. C. Dooling, L. Emery, V. Sajaev, Y. P. Sun

Argonne National Laboratory, Lemont, IL, USA

Abstract

APS has been developing superconducting undulators for over a decade. Presently, two planar and one helical device are in operation in the Advanced Photon Source (APS) storage ring, and a number of devices will be installed in the APS Upgrade ring (APS-U). All superconducting devices perform with very high reliability and have very minor effect on the storage ring operation. To achieve this, a number of storage ring modifications had to be done, such as introduction of the beam abort system to eliminate device quenches during beam dumps, and lattice and orbit modifications to allow for installation of the small horizontal aperture helical device with magnet coils in the plane of synchrotron radiation.

INTRODUCTION

The APS has been developing superconducting undulators (SCUs) for over a decade [1]. SCUs provide a higher peak field on axis for a given undulator gap and period length [2, 3]. Two planar and one helical SCU are in operation in the APS [4, 5]. All of the SCUs are highly reliable and minimally impact APS operations, including the quality and stability of the storage ring electron beam.

It is noted that in the worldwide landscape, SCUs are in operation only at APS and at Karlsruhe Research Accelerator, Karlsruhe Institute of Technology (KIT)/Noell [6, 7]. All of these devices use niobium titanium (NbTi) conductors, and all devices are cooled to ~4 K using cryocoolers. The APS devices include a closed-loop liquid helium (LHe) circuit.

Technical details of the APS SCU designs have been published elsewhere [1, 4, 5, 8, 9]. In this paper, we describe the operational experience with, and integration of, the SCUs into the APS storage ring.

OPERATIONAL HISTORY

After the first 0.33-m-long, 16-mm period superconducting undulator (SCU) was successfully developed, installed, and commissioned in APS in 2013 [1,10], two 1.1-m-long, 18-mm period planar SCUs [4] and a 1.2-m-long, 31.5-mm period helical SCU (HSCU) [5] have been installed and are presently in operation. An extensive beam commissioning plan was executed for SCU0: the equivalent of 5 days [10]. Lessons learned allowed for more compressed commissioning plans for the next devices: the equivalent of 1-2 days. All SCUs were turned over to the beamline for operations immediately after its commissioning period, and all have been very reliable.

The basic operational history for each device (through August 2019) is shown in Table 1. The device operational names are listed; the formal names are in the footnote. SCU operation (power and excitation current) is controlled by the individual beamline. The availability is expressed as the ratio of SCU operating hours relative to the sum of the SCU operating hours and device downtime. The operation percent is given by the ratio of the total hours of SCU operation relative to the total hours of APS user beam delivered (APS delivers just under 5000 hours per year). It is noted that the beamline operating SCU6 was down in calendar year 2019, and user demand for HSCU has been relatively low so far; this explains the lower operation ratios for these two devices. Detailed operational statistics can be found in [11].

Table 1: Basic Operational History of SCUs at APS

Device name	Operation period	Availability	Operation	# Quenches beam/self
SCU0	Jan. 2013-Sep. 2016	98.9%	92.3%	98/6
SCU1[1]	May 2015[3]	99.992%	96.6%	40/5
SCU6[2]	Sep. 2016[3]	99.89%	84.9%	32/3
HSCU	Jan. 2018[3]	100%	14%	0/0

[1] Also known as SCU18-1
[2] Also known as SCU18-2
[3] Presently in operation

The last column in the table shows the total number of times each device quenched during APS operation. A quench refers to the sudden loss of superconductivity when the temperature of any part of the SCU magnet coil windings is raised above the superconductivity threshold temperature. As a result, the windings suddenly develop a finite resistance. A quench detection interlock shuts off the power supply, and the coil heating causes a sudden boil-off of the liquid helium (LHe), which temporarily raises the LHe tank pressure [8]. Quenches are transparent to APS operation.

There are two types of quenches. The majority of quenches are caused when the Machine Protection System (MPS) dumps the stored beam due to a machine fault unrelated to the SCU; the number of instances is given by the first number in the last column in the table. The devices typically recover rapidly [4]; i.e., the magnet temperatures return to ~4 K and the LHe tank pressure reduces to operational levels, such that the devices can be re-energized after the stored beam is recovered. The controls system monitors the status and automatically restores the excitation current if the device is ready. This rapid recovery, 30-45 min. overall, and automation minimizes the device downtime. The second type of quench is when the device quenches while the beam is stored; this is referred to as a

---

MOZBA2

self-quench and the number of instances is given by the second number in the last column in the table. For all four devices, no self-quench has ever caused the stored beam to be lost, and perturbation of the stored beam is minimal, as designed. There is more discussion on quenches later.

INTEGRATION OF PLANAR SCUS

An important criterion for any insertion device (ID), including the SCUs, is that it not degrade the APS storage ring operation below an acceptable level. IDs can affect the storage ring beam through magnetic field errors and by introducing small physical apertures. Small physical aperture and nonlinear field errors could negatively affect injection efficiency, electron beam lifetime, and accumulation of high charge in a single bunch. First- and second-field integral errors could negatively affect stable operating parameters (e.g., beam orbit, tunes, etc.).

Physical Aperture

The SCU0 chamber vertical full aperture (7.2 mm) is similar to that of the vacuum chamber for an APS hybrid permanent magnet (HPM) ID (7.5 mm). To accommodate the SCU0, a standard 4.8-m-long HPM ID chamber was replaced with a half-length ID chamber. A special transition from the ID to SCU0 chamber was designed, using a small-aperture gate valve and bellows. This gate valve and bellows are outside the SCU0 cryosystem. In order to mitigate risk to APS operations, a test chamber was pre-installed with the same aperture, and in the same location, as SCU0 in May 2012. The SCU0 test chamber performed as expected. However, due to an oversight, there was no rigorous reviews of the special transition. The heat load from the beam image currents melted the rf liner of the bellows.

The vacuum transition was changed for the SCU0 installation. Two transitions were added and a standard-aperture gate valve and bellows were used between the upstream HPM ID and the SCU. No further vacuum issues occurred when the SCU0 was installed in Jan. 2013. All SCU designs now avoid gate valves or bellows at small apertures.

Another potential concern is long-term drift of the vacuum chamber position. The cold mass is suspended using Kevlar strings, and the vacuum chamber is attached to the cold mass [1, 12]. The chamber position could change with time, which could negatively affect the vertical aperture in particular. The electron beam was used to measure the vertical position of the vacuum chamber over time [13]. The chamber temperature is sensitive to the beam position, which allows measurement of the relative position of the beam and chamber with high accuracy. Over the first 18 months of operation, SCU0 showed a small vertical position change of < 0.2 mm. A design modification in the cold mass suspension [4] was implemented in next device (SCU1) that reduced the size of the long-term drift by an order of magnitude.

Magnetic Performance

The strongest effect expected from IDs is on the beam orbit through changing field integrals when a device gap (or current) changes. Requirements are given on device field integral errors to limit the effect [1,4]. The field quality of the SCUs is met through precise placement of the windings, precision machining of the magnet cores, and internal correction coils [1,4]. Feedforward (FF) tables combined with orbit feedback then ensure that the devices do not perturb beam orbit.

All SCUs are transparent to user operation after applying corrections. The SCU0 FF table required skew quadrupole correction due to the effect on the beam coupling, but SCU1, SCU6, and HSCU did not. Measurements in the lab [14] of the change in the first-field integral with excitation current agreed well with measurements made with the beam [1].

It was anticipated that SCUs could self-quench during user operation. In case of a quench, the SCU field integrals can change substantially in < 0.1 s. This could lead to a beam dump if the resulting orbit excursion at any ID were to exceed the machine protection limits (±2 mm in X and ±1 mm in Y). In magnetic measurements, all SCUs satisfy the requirement on the maximum allowable field integral change during a quench [1, 4, 5].

During commissioning, the beam orbit was measured at all ID locations during a quench induced with internal heaters on the SCU magnet cores. The main effect is in the horizontal plane. With fast orbit feedback turned off, the maximum horizontal orbit excursion was ±0.6 mm, and with fast orbit feedback turned on (normal user operation), the maximum excursion was about ±0.1 mm [4]. As designed, during the total 14 self-quenches, the stored beam was never lost.

Beam Effects on the SCU

Beam-induced heating is a unique challenge for SCUs, The electron beam generates a heat load on the SCU vacuum chamber from three sources:

- Synchrotron radiation from the upstream dipole (6.6 kW for 7 GeV beam energy and 100 mA current).
- Beam image-current heating.
- Higher-order mode heating in transitions.

Beam heating needs to be accurately predicted in order to design adequate cooling for the SCU. Ray tracing and analytical calculations were used to compute the synchrotron radiation power incident on the SCU vacuum chamber walls for nominal and missteered electron beam. Detailed photon tracking confirmed analytical estimates [15]. Heating by beam-driven higher-order modes in the vacuum transition upstream of the SCUs (described above) was computed using CST Microwave Studio [16]. Power dissipation is predominantly at the gate valve; therefore, there is minimal heat leak into the SCU.

The planar SCU vacuum chamber is designed to allow most of the high-energy photons to pass; only 0.2 W intercepts the walls. Image-current heating on the 20-K aluminum chamber walls, including the anomalous skin effect, was computed to be 4.7 W [17], so this source dominates. The measured chamber temperature with beam was within 1 degree kelvin of the expected temperature. Calibrated chamber heaters were used to correlate power with temperature.

Abort Kicker

As discussed earlier, the SCUs often quench during beam dumps. Such quenches have no effect on operations. However, to minimize the impact on the device, a dedicated abort system was implemented to redirect beam losses away from the devices [18, 19]. This scheme was inspired by quench mitigation implemented for superconducting wigglers [20].

In the original APS beam dump process, the rf drive is removed and the beam loses energy to synchrotron radiation until most of the beam is lost on the smallest inboard half aperture of 15 mm at ID4. However, there are enough electrons lost locally, with enough energy carried by scattered electrons through the vacuum chamber, to heat up the magnet coils. Estimates show that 0.1-1 nC (0.03%-0.3% of the total stored beam charge) reaching the coils is enough to cause a quench [19].

Simulations were used to design the beam abort process. A horizontal kicker was modified to serve as a dedicated beam abort kicker. The pulse was stretched to last for several turns. Beam bunches near the peak of the pulse get kicked out on the first turn, and beam bunches on the rise of the pulse get kicked out on the second turn. To improve the localization of losses, the kicker is fired with some delay after the rf drive is taken away. Since the abort system was implemented, most of the beam is now lost on the injection septum, the second smallest horizontal aperture after ID4. In the first year, the SCU0 quench rate decreased from 80% to 14% of beam dumps. Fiber-optic beam loss monitors mounted at the SCUs [21] show that with the abort system, the local losses after a beam dump can be reduced by an order of magnitude at SCU1 and SCU6 [19].

INTEGRATION OF HELICAL SCU

The HSCU presented a unique challenge, given the small horizontal aperture of the vacuum chamber. Another challenge is that the beam chamber can only be cooled at the ends, leading to a greater temperature rise at the center, compared to the planar devices.

Lattice Change

HSCU vacuum chamber is the smallest horizontal aperture in the APS storage ring: ±13 mm. To make its acceptance larger than the two next-smallest acceptances in the ring, the horizontal beta function at the device had to be reduced from 20 m to 9 m. Multi-objective genetic optimization [22] was used to design the lattice without impact on lifetime or injection efficiency. The lattice was first tested before any hardware modifications. Figure 1 shows the modified lattice functions at the HSCU location.
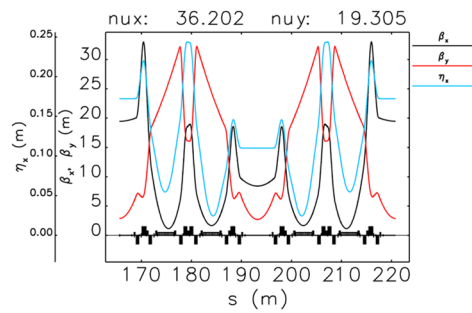
Figure 1: Reduced lattice functions at the HSCU location.

Test Chamber

Unlike planar devices, the HSCU chamber cannot be fully protected from synchrotron radiation heating, which is, in this case, the dominant heat load.

Prior to HSCU installation, a test chamber with identical 13×4 mm half aperture and cross section (shown in Fig. 2) was installed in the APS ring. Similar to the planar chambers, calibrated heater wires were used to calibrate power with temperature; the measurements are shown in Fig. 3.

Beam heating was estimated for the test chamber, assuming 24 bunches; the results are shown in Table 2. For synchrotron radiation, it is assumed that all incident photons are absorbed. For the resistive wall power, room temperature resistivities of $3.2×10^{-8}$ Ω m for Al, and $77.7×10^{-8}$ Ω m for SS, were used.
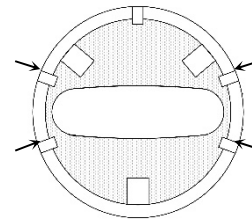
Figure 2: HSCU test vacuum chamber cross section. Heater wires were installed in the four marked machined groves.
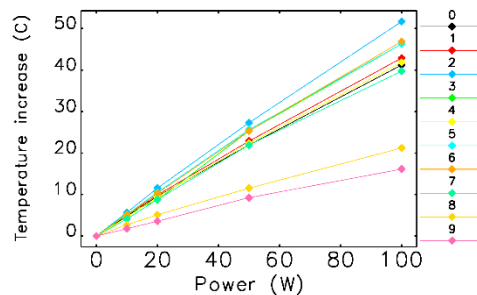
Figure 3: Temperature increase as a function of heater power at all ten sensors [data courtesy M. Kasa].

Table 2: Predicted Beam Power on HSCU Test Chamber

Beam current (mA)	Synchrotron radiation[1] (W)	Resistive wall, Al (W)	Resistive wall[2], SS (W)	Total[3]
25	7.2	0.8	0.2	8.2
50	14.4	3.2	0.9	18.5
100	28.9	13.0	3.5	45.4

1 Only on Al; SS transitions are shielded. Dipole fringe field is included.
2 Average full height of 15 mm used.
3 Thermal diffusion and conductivity differences are not included.

The chamber temperatures were then measured with 24 uniformly-filled bunches, shown in Fig. 4. The heat load from the beam was found to be in reasonable agreement with predictions. The total predicted heat load was 45 W at 100 mA, while the measurements gave 30-40 W. For the cold HSCU chamber, the synchrotron radiation heat load is the same, but the resistive heat load is lower because the resistivity at low temperature is reduced. Therefore, the assumptions in Table 2 are conservative.

Compton Scattering

After HSCU was installed, unexpected heating of the magnet coils was observed with beam, but the vacuum chamber temperature rise was consistent with < 40 W incident power. The magnet coils exceeded 6 K at 80 mA (operational current is 100 mA). The cooling capacity was clearly exceeded because the LHe pressure was rising. The magnet temperatures did not depend on the chamber temperature during scans of the bump in Fig. 5, showing that the magnet heating was not caused by chamber heating. Furthermore, the magnet heating did not depend on bunch pattern (which changes the resistive-wall heating), pointing to synchrotron radiation as the source.
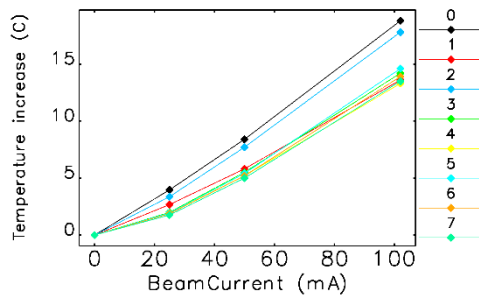
Figure 4: Temperature increase as a function of beam current in 24 bunches at eight of ten sensors (on Al).
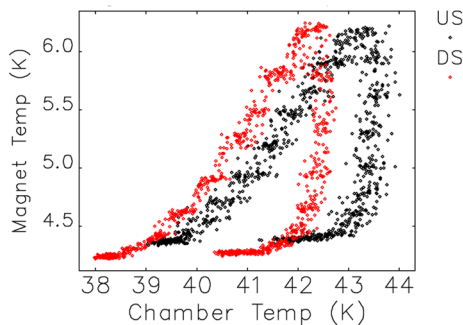
Figure 5: HSCU chamber vs. magnet temperature.

During preparations for HSCU installation, we had anticipated potential issues with radiation heating, considering only small-angle scattering of high-energy photons incident on the wall. An orbit bump was designed ahead of time that reduces the heat load on the chamber by steering the beam in the upstream dipole. When the orbit bump was applied, the magnet temperature showed a strong dependence on amplitude, shown in Fig. 6. The orbit bump was later optimized to utilize dipole trims (Fig. 7), which reduced the size of the orbit bump at the sextupoles, while at the same time increasing the exit angle at the dipole from 0.3 mrad to 0.5 mrad.
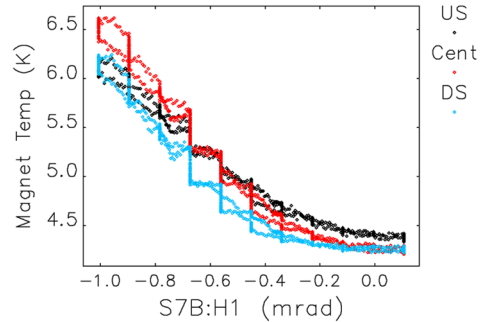
Figure 6: Magnet temperature vs. kick (bump) amplitude.
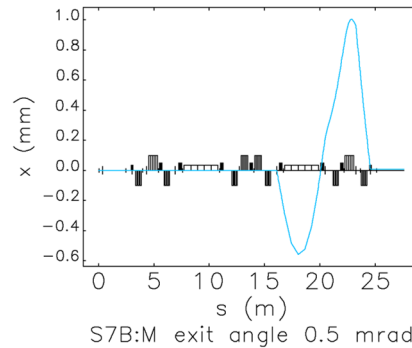
Figure 7: Bump using dipole trim. HSCU location is at far right.

The literature [23] shows that Compton scattering is the dominant effect in photon interaction with aluminum at 100 keV and above. Compton scattering in this energy range can result in large-angle events that significantly reduce the path length of scattered photons through the vacuum chamber.

Post-factum simulations with MARS [24] confirmed this hypothesis. Results show that 2-3 W of synchrotron radiation could be scattered into the HSCU magnet coils, depending on the average energy of the photons [25]. The principle transfer mechanism for photon energies in the dipole radiation spectrum is Compton scattering. Simulations also show that lowering the average photon energy (Fig. 8) (e.g., by steering the electron beam) is an effective method to reduce the fraction of Compton-scattered power reaching the magnet, as observed experimentally. These power levels are consequential to operation of the HSCU.

The orbit bump moves the radiation that reaches the chamber into the dipole fringe field and, therefore, into a softer energy range (Fig. 9). The total radiation power on

the chamber is also reduced from ~20 W with no bump to ~10 W with the bump. The HSCU is presently in operation with the orbit bump and does not experience any issues.
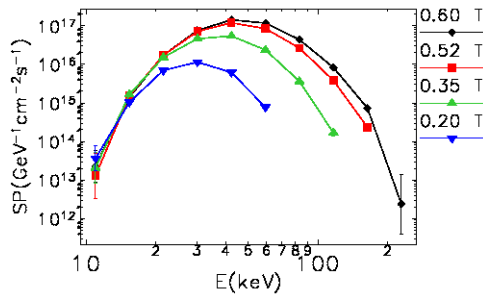
Figure 8: Spectra of photons exiting Al vacuum chamber as a function of dipole field, modeled with MARS.
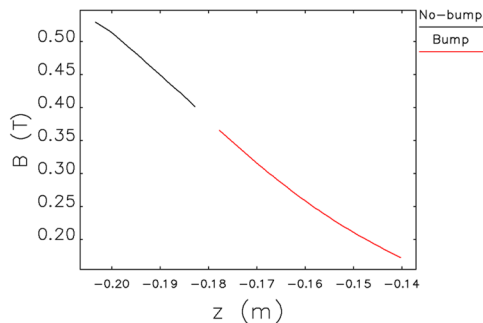
Figure 9: Dipole field for synchrotron radiation incident on HSCU chamber, comparing bump and no bump.

CONCLUSION

Superconducting undulators have been successfully operated at APS since 2013. The SCUs do not degrade APS operation. The effect on the beam orbit is controlled using feedforward, like any HPM ID. The heat load on the planar SCU vacuum chamber matches predictions well. An abort kicker reduces beam-dump-induced quenches, and self-quenches (~once a year per device) do not dump the stored beam. HSCU installation required a lattice change due to the small horizontal aperture. The HSCU showed unexpected heating of the coils attributed to Compton scattering. This heating was mitigated using an orbit bump in the upstream dipole.

Given the successful operational experience with SCUs at APS, SCUs are included the APS Upgrade project [26]. The status of SCU development for APS Upgrade and beyond is described elsewhere [11, 27].

ACKNOWLEDGEMENTS

REFERENCES

[1] Y. Ivanyushenkov, K. Harkay *et al*., "Development and Operating Experience of a Short-Period Superconducting Undulator at the Advanced Photon Source," *Phys, Rev. ST Accel. Beams*, vol. 18, 2015, p. 040703. doi:10.1103/ PhysRevSTAB.18.040703

[2] J. Bahrdt and Y. Ivanyushenkov, "Short Period Undulators for Storage Rings and Free Electron Lasers," *J. Phys. Conf. Ser.: 11th Int. Conf. on Synchr. Rad. Instrum*., vol. 425, 2013, p. 032001. doi:10.1088/1742-6596/425/3/032001

[3] J. Bahrdt and E. Gluskin, "Cryogenic Permanent Magnet and Superconducting Undulators," *Nucl. Instrum. Meth. Phys. Research A*, vol. 907, 2018, pp. 149–168. doi:10.1016/ j.nima.2018.03.069

[4] Y. Ivanyushenkov, K. Harkay *et al*., "Development and Operating Experience of a 1.1-m Superconducting Undulator at the Advanced Photon Source," *Phys. Rev. Accel. Beams*, vol. 20, 2017, p. 100701. doi:10.1103/PhysRevAccel-Beams.20.100701

[5] M. Kasa *et al.*, "Design, Construction, and Magnetic Field Measurements of a Helical Superconducting Undulator for the Advanced Photon Source", in *Proc. 9th Int. Particle Accelerator Conf. (IPAC'18)*, Vancouver, Canada, Apr.-May 2018, pp. 1263-1265. doi:10.18429/JACoW-IPAC2018-TUPMF008

[6] S. Casalbuoni, *et al*., "Superconducting Undulators: From Development towards a Commercial Product," *Synchr. Rad. News*, vol. 31, no. 3, 2018, pp. 24-28. doi:10.1080/ 08940886.2018.1460171

[7] S. Casalbuoni, *et al*., "Commissioning of a Full Scale Superconducting Undulator with 20 mm Period Length at the Storage Ring KARA," *AIP Conf. Proc.*, vol. 2054, 2019, p. 030025. doi:10.1063/1.5084588

[8] J. Fuerst *et al*., "Cryogenic Performance of a Cryocoolercooled Superconducting Undulator," *AIP Conf. Proc.*, vol. 1573, 2014, p. 1527. doi:10.1063/1.4860888

[9] J. Fuerst *et al*., "A Second-Generation Superconducting Undulator Cryostat for the APS," *IOP Conf. Ser.: Mater. Sci. Eng.*, vol. 278, 2017, p 012176. doi:10.1088/1757-899X/278/1/012176

[10] K. C. Harkay *et al.*, "APS Superconducting Undulator Beam Commissioning Results", in *Proc. North American Particle Accelerator Conf. (NAPAC'13)*, Pasadena, CA, USA, Sep.-Oct. 2013, paper WEOAA3, pp. 703-705.

[11] M. Kasa *et al.*, "Status of the Superconducting Undulator Program at the Advanced Photon Source", presented at the North American Particle Accelerator Conf. (NAPAC'19), Lansing, MI, USA, Sep. 2019, paper TUPLH01, this conference.

[12] J. M. Penicka *et al.*, "Alignment of Superconducting Undulators at APS," in *Proc. 13th Int. Workshop on Accel. Alignment (IWAA2014)*, Beijing, China, Oct. 2014.

[13] K. C. Harkay *et al.*, "Beam-based Alignment of the First Superconducting Undulator at APS", in *Proc. North American Particle Accelerator Conf. (NAPAC'13)*, Pasadena, CA, USA, Sep.-Oct. 2013, paper WEPSM07, pp. 1058-1060.

[14] C. L. Doose and M. Kasa, "Magnetic Measurements of the First Superconducting Undulator at the Advanced Photon Source", in *Proc. North American Particle Accelerator Conf. (NAPAC'13)*, Pasadena, CA, USA, Sep.-Oct. 2013, paper THPBA06, pp. 1238-1240.

MOZBA2

[15] L. E. Boon, "Beam-Induced Radiation Heating on the Superconducting Undulator at the Advanced Photon Source, Ph.D. thesis, Dept. of Phys., Purdue University, West Lafayette, IN, USA, 2014.

[16] CST Studio Suite, https://www.solidworks.com/partner-product/cst-studio-suitetm-3d-import-token

[17] K. C. Harkay *et al.*, "Beam-Induced Heat Load Predictions and Measurements in the APS Superconducting Undulator", in *Proc. North American Particle Accelerator Conf. (NAPAC'13)*, Pasadena, CA, USA, Sep.-Oct. 2013, paper WEPSM06, pp. 1055-1057.

[18] K. C. Harkay *et al.*, "Development of an Abort Kicker at APS to Mitigate Beam Loss-induced Quenches of the Superconducting Undulator", in *Proc. 6th Int. Particle Accelerator Conf. (IPAC'15)*, Richmond, VA, USA, May 2015, pp. 1787-1790. doi:10.18429/JACoW-IPAC2015-TUPJE066

[19] K. C. Harkay, J. C. Dooling, V. Sajaev, and J. Wang, "Operational Experience With Beam Abort System for Superconducting Undulator Quench Mitigation", in *Proc. North American Particle Accelerator Conf. (NAPAC'16)*, Chicago, IL, USA, Oct. 2016, pp. 890-893. doi:10.18429/JACoW-NAPAC2016-WEPOB05

[20] W. A. Wurtz, L. O. Dallin, M. J. Sigrist, J. M. Vogt, and M. S. de Jong, "Preventing Superconducting Wiggler Quench during Beam Loss at the Canadian Light Source", in *Proc. 5th Int. Particle Accelerator Conf. (IPAC'14)*, Dresden, Germany, Jun. 2014, pp. 1992-1994. doi:10.18429/JACoW-IPAC2014-WEPRO023

[21] J. C. Dooling, K. C. Harkay, V. Sajaev, and H. Shang, "Operational Experience with Fast Fiber-Optic Beam Loss Monitors for the Advanced Photon Source Storage Ring Superconducting Undulators", in *Proc. North American Particle Accelerator Conf. (NAPAC'16)*, Chicago, IL, USA, Oct. 2016, pp. 28-31. doi:10.18429/JACoW-NAPAC2016-MOA3CO04

[22] M. Borland, V. Sajaev, L. Emery, A. Xiao, "Multi-Objective Direct Optimization of Dynamic Acceptance and Lifetime for Potential Upgrades of the Advanced Photon Source," Argonne, IL, USA, Rep. ANL/APS/LS-319, Aug. 2010.

[23] https://physics.nist.gov/PhysRefData/Xcom/Text/chap4.html

[24] N.V. Mokhov *et al.*, "MARS15 Code Development Driven by the Intensity Frontier Needs," *Prog. Nucl. Sci. Technol.*, vol. 4, 2014, pp. 498-501. https://mars.fnal.gov

[25] J. C. Dooling, R. J. Dejus, and V. Sajaev, "Synchrotron Radiation Heating of the Helical Superconducting Undulator", in *Proc. 10th Int. Particle Accelerator Conf. (IPAC'19)*, Melbourne, Australia, May 2019, pp. 4328-4331. doi:10.18429/JACoW-IPAC2019-THPTS093

26] Advanced Photon Source Upgrade Project Preliminary Design Report, 2017. doi:10.2172/1423830

[27] Y. Ivanyushenkov *et al.*, "Status of the Development of Superconducting Undulators at the Advanced Photon Source", in *Proc. 8th Int. Particle Accelerator Conf. (IPAC'17)*, Copenhagen, Denmark, May 2017, pp. 2499-2502. doi:10.18429/JACoW-IPAC2017-WEOCA3